

Chapter 5: Optical aberrations in the mouse eye

Resumen capítulo 5:

Aberraciones ópticas en ojos de ratón.

El ojo de ratón es un modelo muy utilizado para el estudio de enfermedades retinianas y presenta potencial para convertirse en un modelo de miopía.

Para el estudio de enfermedades de la retina es importante mejorar la obtención de imágenes del fondo de ojo en vivo. Por otro lado, modelos experimentales de miopía se basan en la manipulación de la experiencia visual. En ambos casos el conocimiento de la calidad óptica del ojo, y en particular de la calidad de imagen retiniana, afectados por las aberraciones intrínsecas al ojo es esencial. En este trabajo medimos las aberraciones oculares en el ratón. Se estudiaron doce ojos de seis ratones C57BL/6 de cuatro semanas de edad. Las medidas fueron realizadas en animales despiertos, sin anestésicar, excepto uno, medido bajo anestesia para estudios comparativos. Las aberraciones de onda se ajustaron a quinto orden en una expansión en Polinomios de Zernike. El equivalente esférico y el astigmatismo se obtuvieron a partir de los términos de segundo orden. La función de transferencia de modulación (MTF) se estimó a partir del mejor foco y en función del foco para calcular la profundidad de foco. Todas las estimaciones fueron realizadas para pupilas de 1.5 mm. Los datos de refracción obtenidos a partir de las medidas del Hartmann-Shack fueron consistentemente hipermétropes (media \pm desviación estándar, 10.12 ± 1.4 D) y se encontró astigmatismo significativo en varios ojos, en promedio 3.64 ± 3.70 D. La aberración esférica era positiva en todos los ojos (0.15 ± 0.07 μm) y la RMS de los términos de coma era alta (0.10 ± 0.03 μm) comparada con la RMS de otros términos de Zernike. La MTF estimada a partir de las aberraciones de onda mostraba una modulación de 0.4 a 2 ciclos/grado en el mejor foco (y 0.15 teniendo en cuenta el desenfoque medido). Para esa frecuencia espacial la profundidad de foco estimada usando el criterio de

Raleigh era de 6 D. Los valores de aberraciones en el ratón anestesiado fueron mayores que en el mismo ojo del animal sin anestesiarse. Los desenfoques hipermetrópicos encontrados en el ojo del ratón en este estudio son consistentes con los datos publicados sobre ratones medidos con retinoscopia. La óptica del ojo del ratón está lejos de ser limitada por difracción con pupilas de 1.5 mm y tiene valores importantes de aberración esférica y coma. De todos modos, las MTFs estimadas a partir de la aberración de onda son mayores que las publicadas con técnicas de doble paso, resultando en una menor profundidad de foco estimada. A pesar de que las aberraciones imponen una degradación importante en la calidad de imagen retiniana, su magnitud no excede valores corregidos típicamente por las técnicas de óptica adaptativa que se podrían utilizar para visualizar el fondo de ojo. Por otro lado, las aberraciones no parecen ser el factor limitante en la resolución espacial del ratón. A pesar de que la óptica del ojo del ratón es mucho más degradada que la de otros modelos experimentales de miopía, su elevada tolerancia al desenfoque no parece estar determinada totalmente por las aberraciones oculares.

This chapter is based on the article by García de la Cera et al. "Optical aberrations in the mouse eye", *Vision Research* (2006) 46, 2546-2553.

The contribution of Elena García de la Cera to the study was to develop the methodology to measure ocular aberrations in mice (optical set-up, calibrations, automatic control, data processing routines), with the adaptations required to the instrument. She also performed the experimental measurements on mice and participated in the data analysis and interpretation.

Coauthors of the study are: Guadalupe Rodríguez, Frank Schaeffel, Christine Schmucker and Susana Marcos.

5.1. Abstract

The mouse eye is a widely used model for retinal disease and has potential to become a model for myopia. Studies of retinal disease will benefit from imaging the fundus in vivo. Experimental models of myopia often rely on manipulation of the visual experience. In both cases, knowledge of the optical quality of the eye, and in particular, the retinal image quality degradation imposed by the ocular aberrations is essential. In this study we measured the ocular aberrations in the wildtype mouse. Twelve eyes from six four-week old black C57BL/6 wildtype mice were studied. Measurements were done on awake animals, one being also measured under anaesthesia for comparative purposes. Wave aberrations were fit to up to 5th order Zernike polynomials. Spherical equivalent and astigmatism were obtained from the 2nd order Zernike terms. Modulation Transfer Functions (MTF) were estimated for the best-focus, and through-focus, to estimate depth-of-focus. All reported data were for 1.5-mm pupils. Hartmann-Shack refractions were consistently hyperopic (10.12 ± 1.4 D, mean and standard deviation) and astigmatism was present in many of the eyes (3.64 ± 3.70 D, on average). Spherical aberration was positive in all eyes (0.15 ± 0.07 μm) and coma terms RMS were significantly compared to other Zernike terms (0.10 ± 0.03 μm). MTFs estimated from wave aberrations show a modulation of 0.4 at 1 c/deg, for best focus (and 0.15 without cancelling the measured defocus). For that spatial frequency, depth-of-focus estimated from through-focus modulation data using the Raleigh criterion was 6 D. Aberrations in the eye of one anaesthetized mouse eye were higher than in the same eye of the awake animal. Hyperopic refractions in the mouse eye are consistent with previous retinoscopic data. The optics of the mouse eye is far from being diffraction limited at 1.5-mm pupil, with significant amounts of spherical aberration and coma. However, estimates of MTFs from wave aberrations are higher than previously reported using a double-pass technique, resulting in smaller depth-of-field predictions. Despite the large degradation imposed by the aberrations they are lower than the amounts of aberrations typically corrected by available correction techniques (i.e adaptive optics). On the other hand

aberrations do not seem to be the limiting factor in the mouse spatial resolution. While the mouse optics are much more degraded than in other experimental models of myopia, its tolerance to large amounts of defocus does not seem to be determined entirely by the ocular aberrations.

5.2. Introduction

The mouse is the most widely used animal model for human diseases, including inherited vision disorders. Its genome has been almost completely sequenced and there are many transgenic models available. For example, mouse models of retinal degeneration have been investigated for many years in the hope of understanding the causes of photoreceptor cell death (Chang et al. 2002). There are also knockout mouse models for cataracts (Hegde et al. 2003), glaucoma (Lindsey and Weinreb 2005), and diabetic retinopathy (Kern and Engerman 1996). Also, there are recent efforts to develop a mouse myopia model by visual deprivation (Beurman et al. 2003; Schaeffel et al. 2004).

Electrophysiological (Porciatti et al. 1999) and behavioral studies (Gianfranceschi et al. 1999; Prusky et al. 2004; Schmucker et al. 2005) indicate that the visual spatial resolution in the wild type mouse is poor, and the debate is open whether the optics of the eye match the coarse resolution of the neural mosaic (Artal et al. 1998). Knowledge of the retinal image quality in the mouse is important for various reasons. First, it will help to clarify the limits of spatial vision in the mouse. Second, the measurement of the aberrations of the mouse eye and their potential correction by means of adaptive optics (Roorda and Williams 2001) or phase-plates (Burns et al. 2002) will open the possibility of applying new *in vivo* retinal imaging methods. *In vivo* observations of critical retinal features in mice with retinal degenerations, glaucoma or diabetic retinopathy will allow a better understanding of the pathogenesis, and longitudinal measurements of associated changes and effects of drug therapies, not possible in the cross-sectional data provided by histology (Marcos et al. 2004; Ritter et al. 2005; Schmucker et al. 2005). However, the current correction technology, and the resolution of the fundus images will be limited by the actual amounts of aberrations present in these eyes. Finally, most frequent myopia models rely on the ability of the ocular growth mechanisms to respond to visual

experience. However, optical aberrations determine to a great extent the depth-of-focus of the eye (Marcos et al. 1999; Marcos et al. 2005), and the effects of defocus on retinal image quality will be drastically different whether the eye is diffraction-limited or highly aberrated.

Despite the need for a clearer understanding on the degradation imposed by the optics of the mouse on the retinal image, there are very limited studies that have attempted to assess it, and none, to our knowledge has measured the optical aberrations in the mouse. The very few studies available suggest that the optics of the rodent eye is highly degraded (Artal et al. 1998). Hughes & Wassle (Hughes and Wassle 1979) reported drastic drop in the contrast of grating targets projected on rat retinas and observed by indirect retinoscopy. Schmucker et.al. (Schmucker and Schaeffel 2004) reported photoretinoscopic reflexes consistent with high amounts of aberrations. A recent report (Irving et al. 2005) shows very distorted Hartman-Shack images and consequently high amounts of aberrations in the awake rat eye. To our knowledge the only published study on the objective retinal image quality of the rodent eye (six 3-month Long Evans rats and three C57BL/6J mice of the same age) was that of Artal et al., using a double-pass system (Artal et al. 1998). Animals were fully anaesthetized. By recording through focus double-pass aerial images of a point source they found very little optical quality change (less than 10%) across 24 D, with a slight tendency of optical quality to increase with hyperopic corrections (although they failed at finding a “best focus”). Large depth-of-focus in the rat eye (± 10 D) had been predicted by Green and coworkers (Green et al. 1980). Remtulla and Hallett (Remtulla and Hallett 1985), based on eye size and photoreceptor diameters predicted a depth-of-focus of ± 56 D in adult mice, or ± 11 D once differences between behavioural and ganglion cell acuity were taken into account. Other studies report ± 10 D from whole-body optomotor responses (Schmucker et al. 2005). Hyperopic defocus has also been reported using streak retinoscopy and IR photoretinoscopy in mice, with refractive states ranging from +15.0 D in adult Balb/CJ mice (Beuerman et al. 2003), +13.5 D in 30-day-old C57BL/6J mice (Tejedor and de la Villa 2003), or +7.0 D in 70-day-old mice by Schmucker et

al. (Schmucker and Schaeffel 2004). These hyperopic refractions do not match however those estimated by visual evoked potentials (Mutti et al. 1997), the potential difference being attributed to relatively large distance between the photoreceptor plane layer and the retinal layer where the retinoscopic reflection potentially takes place.

The only experimental modulation transfer functions (MTFs) available in the rodent eye (mostly rat's and one example for one mouse) are those from Artal et al.'s study (Artal et al. 1998) on anaesthetized animals. This study reports modulations of less than 0.1 for the mouse and 1 for the rat at 1 c/deg, for 1-mm pupils. In the double-pass method MTFs are estimated from the intensity distributions of the aerial images of a point source reflected by the retina, and therefore highly dependent on retinal scattering. It is questionable however whether this veiling pedestal affecting the double-pass aerial image truly represents the actual point spread function of the ocular optics. Provided that the ocular media are clear, and intraocular scattering is not a major source of retinal image degradation, MTFs obtained from wave aberrations will account for the actual contrast losses caused by the ocular optics in the mouse, unaffected by retinal scattering. In addition, the measurement of individual aberrations in the mouse eye will allow us to better understand the sources of optical degradation. A previous study (Artal et al. 1998) attempted to predict aberrations in the rat eye using a simple eye model and biometric data provided by Hughes (Hughes 1979). Those simulations found significant amounts of spherical aberrations due to the highly curved surfaces of small eyes. However the predicted MTFs were higher than the experimental MTFs that let the authors to conclude that other unknown high order aberrations were also present. Currently, new biometric data in the mouse are available using new technology (Lin et al. 2004; Schmucker and Schaeffel 2004). Predictions based on eye models could be revisited in the light of those newly reported biometric data and the ocular aberrations reported here and it will be addressed in this thesis in Chapter 6. Finally, measurements of the wave aberrations will allow us to obtain the refractive state of mice, from the defocus term in the polynomial expansion describing the wave aberration function, and also to estimate the depth-of-

focus, by computing through-focus optical quality as the defocus term is computationally changed in the wave aberration function.

In this chapter we present measurements of ocular aberrations (low and higher order) in the wild type mouse. The aims of the study were to investigate:

- 1) Ocular aberrations and retinal image quality in the mouse eye
- 2) The optical depth-of-focus in the mouse eye
- 3) Relationships between ocular aberrations and refractive error in the mouse eye

This experiment could reveal if ocular aberrations in mice have any effect in ocular development and their consequences in the potential of mouse as myopia model.

5.3. Methods

5.3.1. Subjects

Black C57BL/6 wildtype mice were obtained from Charles River, Barcelona, Spain and kept in the animal facilities of the Instituto de Oftalmobiología Aplicada, Universidad de Valladolid, Spain, housed in standard mouse cages under 12 hours light/dark cycle. All experimental protocols were approved by the Institutional Review Boards, and met the ARVO resolution for care and use of laboratory animals. Six four week old females were used in this study.

5.3.2. Hartmann-Shack aberrometer

Ocular aberrations were measured with a Hartmann-Shack aberrometer built at the Instituto de Optica (Consejo Superior de Investigaciones Cientificas), Madrid, Spain, described in Section 2.1.1. The particularly low quality of the Hartmann-Shack spots from mouse eyes prevented to use the more standard processing algorithms developed previously. Therefore new routines for HS spot detection, and centroiding algorithms were written in Matlab (Mathworks, Natick MA) and specifically developed for the present study. Zernike coefficients were obtained by modal fitting of the lateral deviations to the derivatives of the Zernike polynomial expansion up to the 5th order.

5.3.3. Experimental protocols

Mice were measured in the Hartmann-Shack system under awake and normal viewing conditions, i.e. without anaesthesia nor with cyclopegia. The animals were restrained by holding their tails while they were sitting on an elevated platform mounted in front of the system, which allowed centration and focusing of the animal's pupil. Figure 5.1 The pupil image channel

provided continuous pupil monitoring and let us controlling Purkinje images from the IR ring during measurements. We made sure that the Purkinje images remained within the pupil, as used this as an indication that fixation was not too eccentric. Additional centration could be achieved by moving the x-y stage that translates the entire Hartmann-Shack system. After some adaptation to the task, the mice became cooperative and did not move during the measurement, allowing us to capture several (5- 10) images per eye. The same procedure was repeated for left and right eyes.



Figure 5.1. Mouse previous to measurements. Animal was placing in a platform in front of the Harman-Shack system near to IR ring LEDs.

For comparative purposes, mouse labelled as # 2 was also measured under anaesthesia . Mouse # 2 were anaesthetized with an subcutaneous injection of a mixture of 1.2ml 10% ketamine hydrochloride and 0.8 ml 2% xylazine hydrochloride, dissolved in 8.0 ml sterile saline. In those measurements eyelids were held open and the cornea was moistened with eye drops (Viscofresh 0.5% ,Allergan).

5.3.4. Data analysis

Typical Hartmann-Shack images contained about 12 spots. In general, images from the same eye were very similar, suggesting a good fixation by the animal. Data were processed for the maximum pupil diameter (ranging from 1.63 to 2.17mm). For comparative purposes, across eyes the minimum pupil diameter of 1.5mm was used. Reported data for each eye are averaged

of at least 5 individual measurements. The optical quality of the eye was assessed in terms of individual Zernike coefficients and the root-mean-square wavefront error (RMS) of the different terms or orders. Modulation Transfer Functions (MTF) and Point Spread Functions (PSFs) were also obtained from the wave aberrations. The volume under the MTF and the modulation at 2 c/deg were also used as an optical quality metric. Through-focus estimates of these metrics were used to compute depth-of-focus.

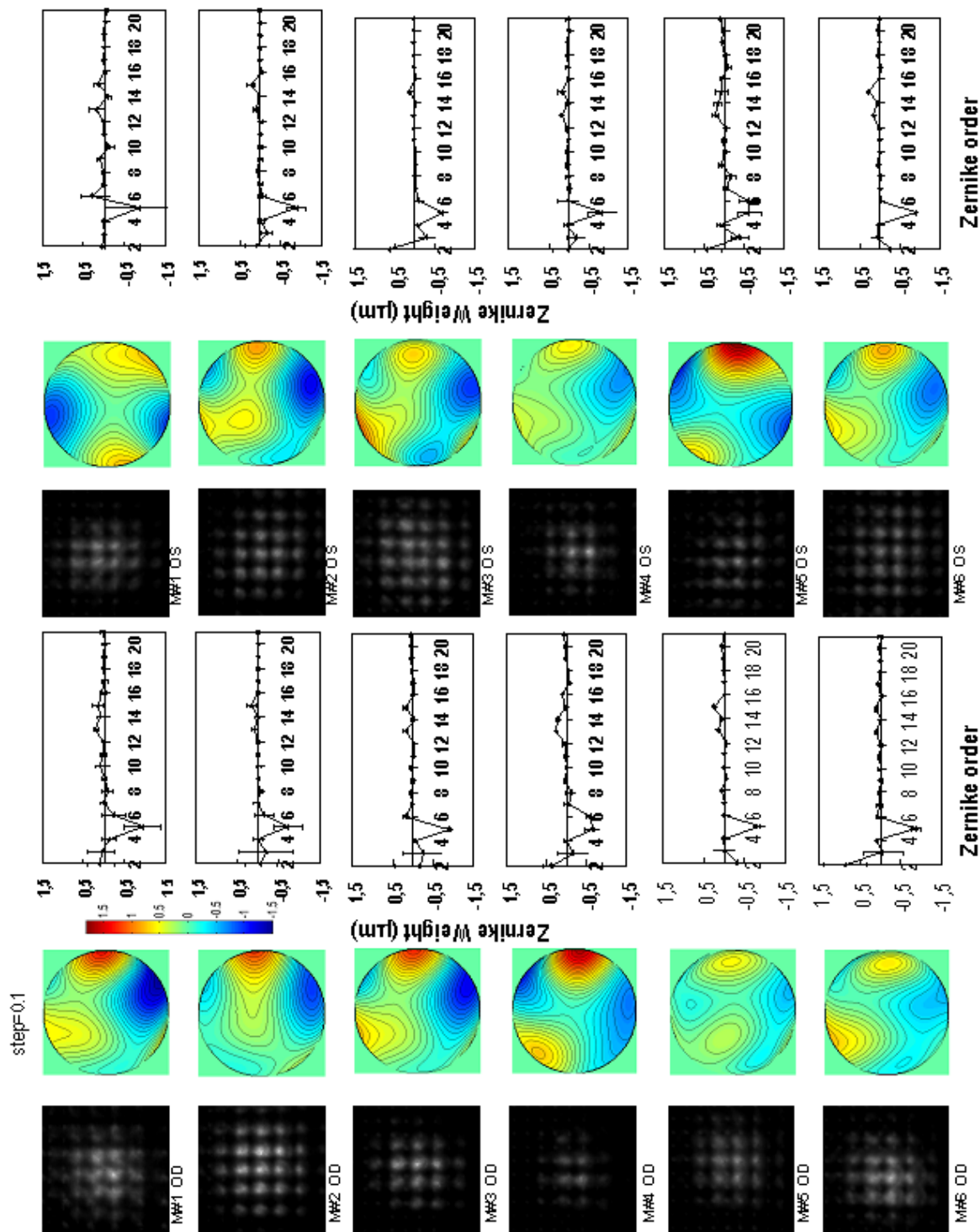


Figure 5.2. Examples of Hartmann-Shack images on awake mouse eyes (scale: 3.4 mm x 3.4 mm), and corresponding wave aberration maps and mean Zernike coefficients. Wave aberration maps are for 3rd and higher order aberrations, and contour lines are plotted in 0.1 μ m steps. Zernike coefficients are ordered following the OSA convention, and the error bars stand for standard deviations. Data are for 1.5-mm pupil diameters

5.4. Results

5.4.1. Hartmann-Shack images and wave aberrations

Figure 5.2 shows the Hartmann-Shack raw data (left), clearly more degraded than those typically found in human eyes (Liang and Williams 1997), chicks (Chapter 3) (García de la Cera et al. 2006), rhesus monkeys (Vilupuru et al. 2004) or cats (Huxlin et al. 2004). The corresponding wave aberrations (center), for 3rd and higher order aberrations (for 1.5 mm pupils) show prevalence of positive spherical aberration in most of the animals, as well as significant amounts of other high order aberrations, even for these small pupil sizes. Zernike coefficients are also shown (right) in all eyes (average across measurements in each eye, and the corresponding standard deviation), following the Optical Society of America notation (Thibos et al. 2000).

5.4.2. Refractive state

Zernike coefficient Z_2^0 , corresponding to the defocus term (with negative sign, consistent with hyperopic defocus), is the largest in all eyes, as shown in Figure 5.2. Figure 5.3 shows the average spherical equivalent found

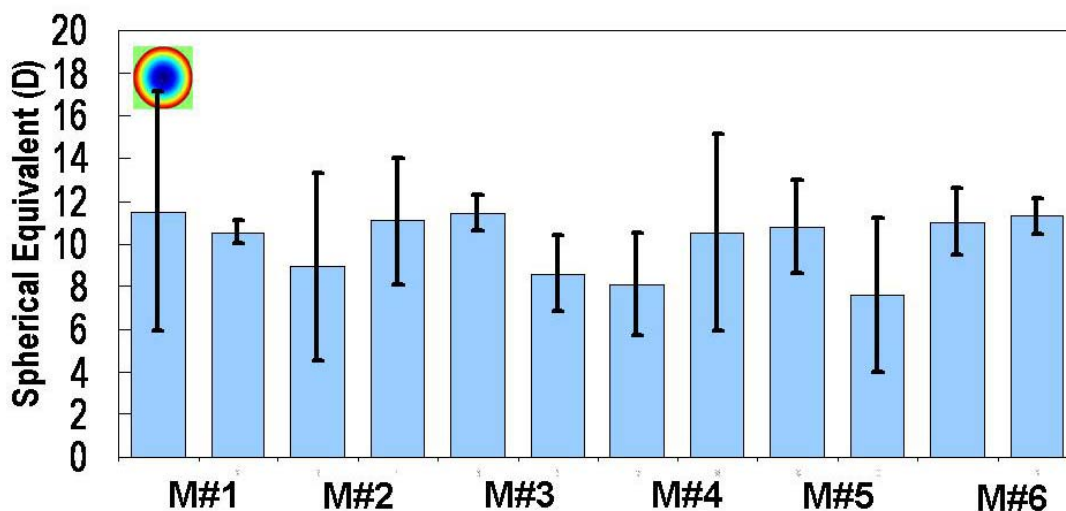


Figure 5.3. Spherical equivalent for all mice. red bars correspond to right eyes and blue bars to left eyes. Error bars stand for standard deviations across measurements.

for each eye, computed from the defocus term of the Zernike polynomial expansion, for a wavelength of 678 nm. The spherical equivalent is consistently hyperopic in all eyes, $+10.12 \pm 1.41$ D (average \pm standard deviation). Intersubject variability is of the order of the average interocular differences (1.97 D) and smaller than the average measurement variability (2.61 D). Astigmatism was computed from Zernike terms Z_2^1 and Z_2^{-1} and found to be on average 3.64 ± 3.70 D. Taking the measured astigmatism into account, pure spherical error resulted in 8.30 ± 3.00 D. We did not find a preference for the horizontal or vertical meridian to be the least hyperopic. The astigmatism axis tended to be mirror symmetric across left and right eyes. Astigmatism axis values are clustered around 37 ± 4 deg and -37 ± 9 deg (or 127 ± 9 deg in the positive cylinder convention) in all eyes except one (#4, left eye).

5.4.3. High order aberrations

Figure 5.4 shows root mean square wavefront errors (RMS) for different terms and all eyes, for 1.5-mm pupils. Average third and higher order aberration RMS is 0.32 ± 0.08 microns. Spherical aberration accounts for a significant proportion of the high order aberrations (0.15 ± 0.06 microns), equivalent to a blur of 1.85 D. However third order aberrations alone (RMS=

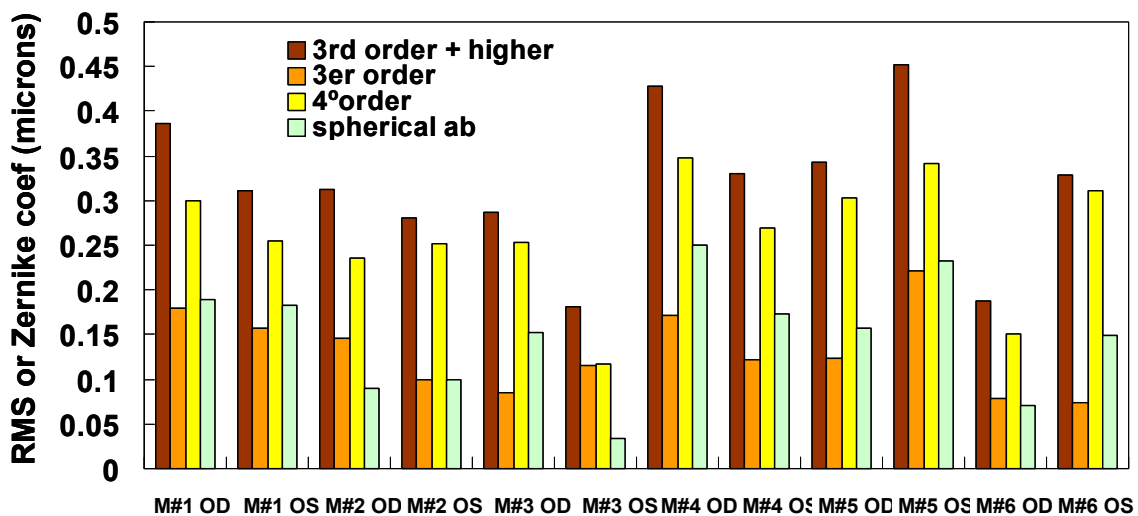


Figure 5.4. Mean 3rd and higher order RMS (black bars), 3rd order RMS (light grey) bars, 4th order RMS (dark grey bars), spherical aberration Zernike coefficient (white bars) and 5th order RMS (dotted bars). Error bars represent intersubject variability and stand for standard deviations across eyes. Data are for 1.5-mm pupil diameters.

0.13 ± 0.04 microns represent also a major source of degradation, particularly coma (RMS= 0.10 ± 0.03 microns). While other non-spherical 4th order terms are important (compare dark gray and dotted bars in Figure 5.4), 5th order terms are not very different from zero (0.09 ± 0.04 microns). High order aberration intersubject variability is low and comparable with variability of repeated measurements on the same eye (0.07 microns, on average).

5.4.4. Modulation Transfer Functions

Figure 5.5 shows average radial-profile MTFs across all eyes obtained from wave aberrations, for 1.5 mm pupils and for the illumination wavelength (678 nm). Average best-focus MTF (i.e. correcting for hyperopic defocus) is shown in black line, and average non-corrected MTF (i.e. with all low and higher order aberrations) is shown in dotted blue line. For proper comparison of MTFs, it should be noted that the mouse eye has a particularly low numerical aperture (NA= 0.5). MTFs for 1.5 mm pupils in another small eye (chick eye, NA= 2.6) from Chapter 3 and the average human eye MTFs for 6.5-mm pupil diameter (NA= 3.4) are also shown for comparison, along with the diffraction-limited MTF for 1.5mm pupils. As a reference, the diffraction-

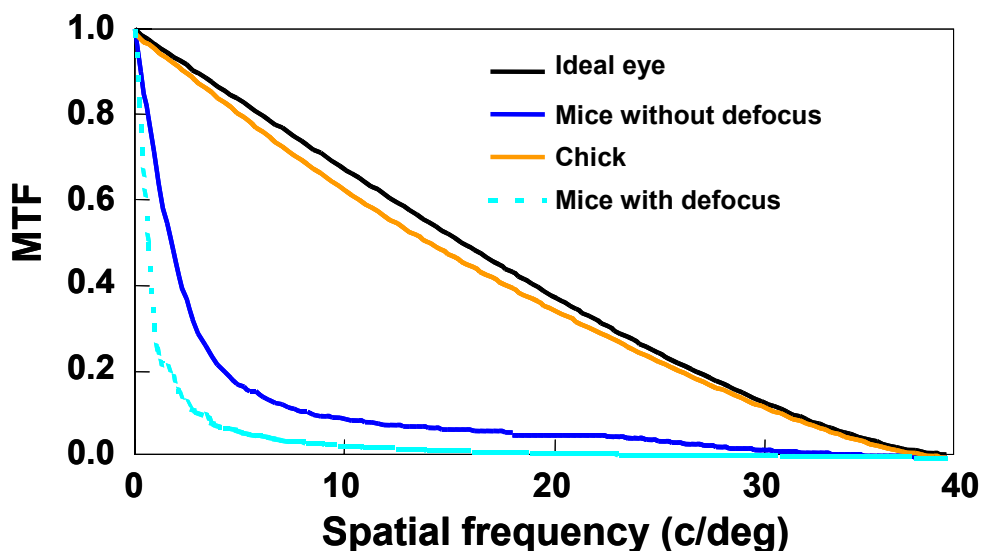


Figure 5.5. Mean MTFs (radial profile) averaged across all mouse eyes for best focus (solid dark blue line), and uncorrected defocus (dotted light blue line) for 1.5 mm pupil diameter. For comparison average MTF for 4-week old chicks (n= 5) for 1.5 mm-pupils (yellow line) from wave aberrations measured with the same Hartmann-Shack system (Chapter 3 and García de la Cera et al. 2006) and the theoretical MTF of a diffraction-limited eye for 1.5-mm pupil is also represented.

limited MTF with the same amount of defocus as found in the mouse eye has also been included. Both the human and chick eyes are nearly diffraction-limited for this pupil size. In the mouse, while defocus imposes additional optical degradation, major losses in contrast are produced by high order aberrations.

5.4.5. Depth-of-focus

Through-focus image quality estimated by computationally changing the defocus term (at 1 D steps) in the wave aberration, for 1.5-mm pupils, is represented in Figure 5.6. Modulation transfer for 2 c/deg (same spatial frequency used by Artal et al. 1998 for the rat eye) was used as an image quality metric. The curves in Figure 5.6 are referred to zero defocus, i.e. compensating the spherical equivalent given by the defocus term in each eye. However, in most eyes, the highest optical quality does not correspond to that correction, as typically found in the presence of high order aberrations (Guirao and Williams 2003). We found best-optical quality to be shifted on

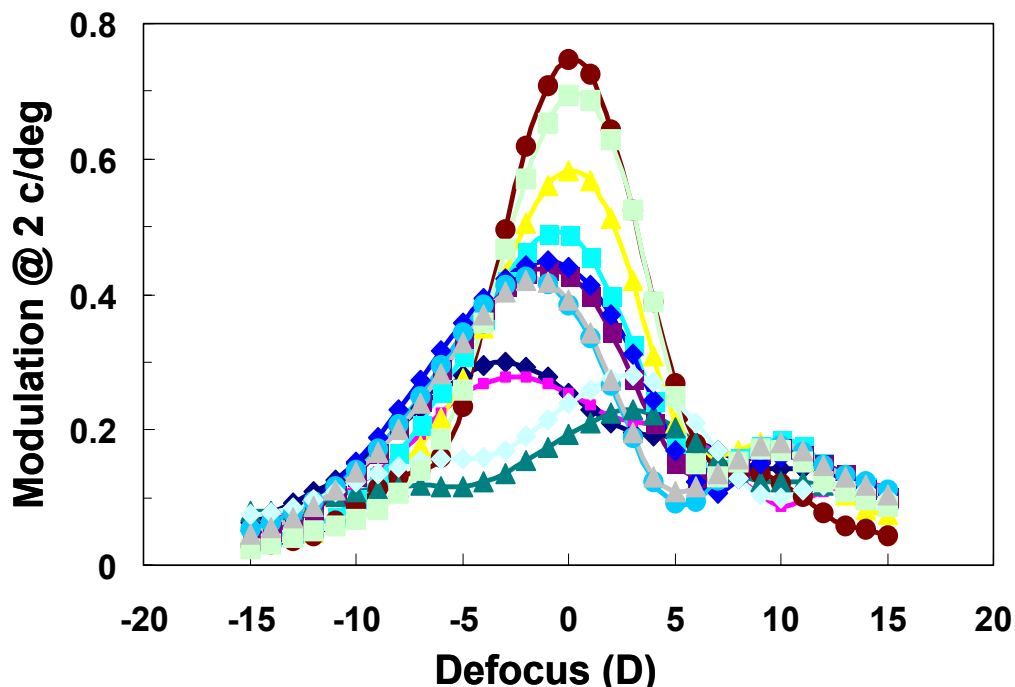


Figure 5.6. Through-focus modulation transfer at 2 c/deg, estimated from radial profile MTFs. Each colour corresponds to a different mouse eye. A positive defocus sign is indicative of positive defocus at the retinal plane (and therefore required myopic correction) and viceversa for negative defocus.

average 0.42 D toward less hyperopic values. Depth-of-focus was estimated using the Raileigh criterion, i.e. as the defocus range for which optical quality was at least 80% of the value at best focus (Marcos et al. 1999) and ranges from 7.9 to +4.5 D. The volume under the MTF was used as another metric to obtain the depth-of-focus, and values ranging from 11 to 1.7 D were found using this metric. We found that depth-of-focus was highly correlated with the amount of individual 4th order spherical aberration present in each eye ($r=0.726$, $p<0.0001$), as shown in Figure 5.7.

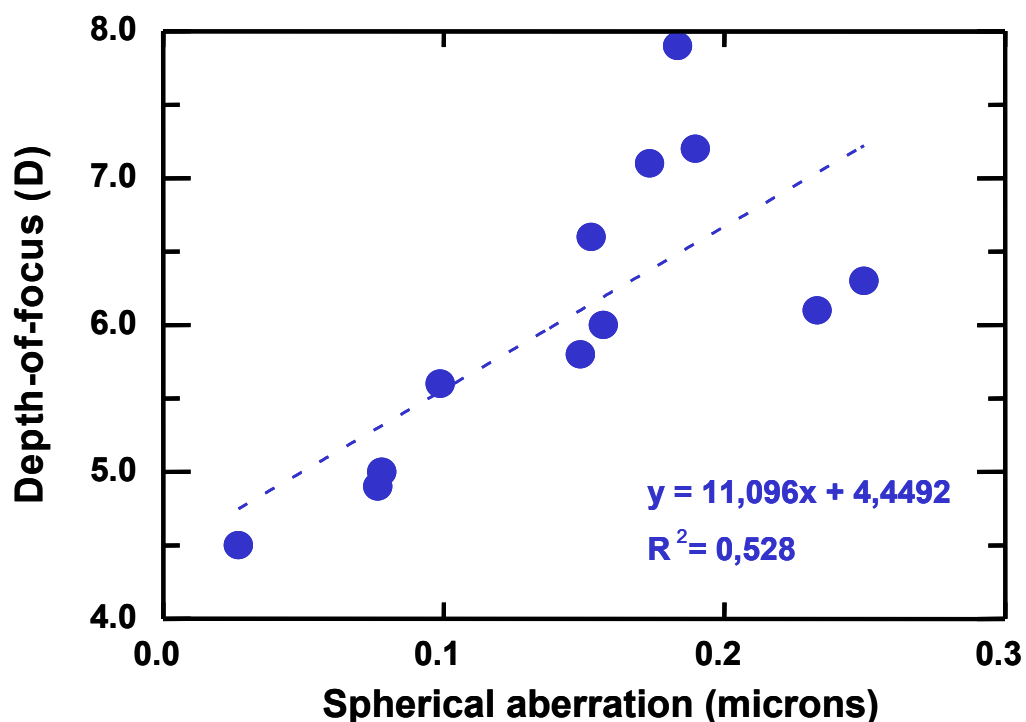


Figure 5. 7. 4th order spherical aberration from Zernike expansion vs. depth-of-focus from through-focus modulation transfer at 2 c/deg using the Raileigh criterion for all eyes. Data are from 1.5 mm pupil diameters.

5.5. Discussion

5.5.1. *The effect of anaesthesia*

While the measurement of the optical quality of the mouse eye under normal viewing conditions is important to get insights on the limits of spatial resolution, and to assess the prospects of the mouse as a myopia animal model, several applications will very likely require the use of anaesthesia to immobilize the animal, for example in vivo retinal imaging. Also, previous measurements of the double-pass MTF in the rodent eye (Artal et al. 1998) were performed under total anaesthesia (Equistesin) (Artal et al. 1998).

We compared measurements with and without anaesthesia on the same eye (right eye of mouse # 2), to assess possible effects of the drug on optical quality. Measurements were attempted on other animals, but rapid opacification of the crystalline lens during anesthesia prevented completion of these measurements. We found larger HS spots in the anaesthetized eye than previous measurements under awake conditions on the same eye. We found higher amounts of aberrations in the anaesthetized eye (RMS for 3rd and higher order was 0.42 microns in the anaesthetized animal vs 0.32 microns in the awake animal; spherical aberration was 0.14 microns vs 0.09 microns; and RMS for 3rd order was 0.32 microns vs 0.15 microns). We also found a lower hyperopic spherical equivalent in the anaesthetized eye (+3.28 D vs +10.12 D).

While these results are only for one eye, they may be indicative of larger optical degradation in anaesthetized mouse eyes, and perhaps a possible cause of the differences in retinoscopic refractions from different authors (Beuerman et al. 2003; Tejedor and de la Villa 2003; Schmucker and Schaeffel 2004). As previously reported other additional complications further deteriorating optical quality under anaesthesia, not accounted for by aberrometric MTFs but very likely decreasing contrast of retinal images are

the corneal dryness and transient cataracts induced by anaesthesia (Calderone et al. 1986).

5.5.2. Comparisons with other studies: refraction, MTF and depth-of-focus

We found hyperopic defocus in the 4-week old mouse eye of $+10.12 \pm 1.41$ D using Hartmann-Shack aberrometry at 680 nm, only slightly higher than those reported by Schmucker & Schaeffel (Schmucker and Schaeffel 2004) for mice of the same age ($+7.0 \pm 2.5$ D) using infrared photoretinoscopy at 880 nm. These results are in contrast to previous studies using streak retinoscopy, reporting larger amounts of hyperopic defocus with eyelid suture (up to $+13.5$ D by (Tejedor and de la Villa 2003)). A control experiment performed by Schmucker & Schaeffel (Schmucker and Schaeffel 2004) demonstrates that chromatic aberration is not the cause for the discrepancy. The fact that the retinal reflection may occur in a retinal layer different from the photoreceptor layer, which is effectively aggravated in eyes with short focal lengths (the so-called “small eye artifact” (Glickstein and Millidot 1970)) and reported differences with refractive errors obtained visually evoked potentials (less hyperopic) leaves the question open of whether the mouse eye is truly hyperopic. Additionally, (Schmucker and Schaeffel 2004) observed ring-shaped intensity distributions of the retinoscopic pupillary images, what led them to suggest that the crystalline lenses might be multifocal, similar to what has been described for fish eyes (Kroger et al. 1999). The spatial sampling resolution of our lenslets (400 microns) is too coarse to draw any conclusion regarding multifocality in the mouse eye.

We have computed MTFs from the measured wave aberrations in the mouse eye, for best focus (i.e. simulating correction of the measured hyperopia) and different amounts of defocus. The average MTF at best focus can be compared with, to our knowledge, the only MTF previously reported, which corresponds to one single mouse eye, using a double-pass technique. While we found generally low MTFs, these are not as severely degraded as the MTF reported by Artal et al. (1998). While that study shows modulations

lower than 0.1 for 2 c/deg for 1-mm, we found modulations close to 0.4 for that spatial frequency (see Figure 5.5), for 1.5 mm pupils. There are several possible reasons for the discrepancy: 1) the previous study performed measurements under anaesthesia, which appears to lower image quality, and presumably increase corneal and intraocular scattering, what the double-pass method is able to capture; 2) double-pass MTFs are likely affected by the presence of retinal scattering, producing halos in the aerial image resulting in a lower MTF; 3) the previous study only reports limited data on a single mouse, even though three animals were used as subjects, and the authors did not mention whether this was due to problems in data processing in the other two animals, or due to other reasons.

On the other hand, the enlarged aerial spots in the Hartmann-Shack images may be suggestive of fine structure in the wave aberration not being resolved by the lenslet array. However, the fact that 5th order aberrations are of much lower magnitude than 3rd or 4th order aberrations indicates that we are probably not overestimating the MTF by not capturing higher order aberrations. The degraded retinal spots may be just indicative of large amounts of retinal scattering.

We have also obtained estimates of optical depth-of-focus, which can be compared with previous predictions and measurements from the literature. As shown by Figure 5.6, the actual depth-of-focus will very much depend on the definition used. We found large depth-of-focus particularly in eyes with larger amounts of spherical aberration. However, our data of optical depth-of-focus are lower than previous predictions and reports using the double-pass method.

5.5.3. *Implications of the results*

Our results confirm previous speculations that higher order aberrations are major sources of optical quality degradation in the mouse eye. Significant amounts of spherical aberrations are consistent with highly curved spherical surfaces, although a complete predictive model should incorporate aspheric surfaces and gradient index distributions in the crystalline lens (and will be shown in Chapter 6). The presence of large amounts of third order aberrations and astigmatism may be due to eccentric fixations with respect to the optical axis. Interestingly, the high repeatability of the measured coma terms and relatively low intersubject variability seems to indicate that mouse use a certain fixation axis or did not make too large eye movements, despite their afoveated retinas.

Even if we found severely degraded optics compared to the diffraction-limit, our MTF estimates for best-correction in the mouse are higher than previously reported using double-pass in one anaesthetized mouse, and even rats. Even with defocus, the modulation at 2 c/deg is 0.2, which indicates that the optics does not impose the limits to spatial vision in the mouse eye. Behavioral and electrophysiological experiments report visual acuities of 0.5-0.6 c/deg (Gianfranceschi et al. 1999; Porciatti et al. 1999). The fact that anaesthetized animals show larger amounts of aberrations than awake animals complicates further their correction for in vivo imaging. Provided that the second order aberrations are corrected by other means, current adaptive optics technology generally provides sufficient stroke to compensate the RMS measured in the anaesthetized animal (0.5 microns). It seems more challenging to generate centroiding algorithms that process the severely degraded Hartmann-Shack in real time (our algorithms are accurate but not time-efficient), and to handle the presence of cataracts and corneal dryness.

The use of the mouse as an animal model for myopia has been challenging. Degrading the optical quality by diffusers (Schaeffel and Burkhardt 2002) or minus-lens power wear (Beuerman et al. 2003) has been shown to change the refractive state in the myopic direction but not all the studies show clear axial elongation. In fact, in one of the studies (Tejedor and de la Villa 2003) the refractive and axial length change did not seem to correspond with each other (Tejedor and de la Villa 2003). Our results show that moderate amounts of imposed spherical defocus (see Figure 5.6) will not alter optical quality significantly, and therefore it is not surprising that mice do not respond to a lens-treatment as easily as other models. However, the measured optical depth-of-focus is lower than estimated from behavioral measurements (Schmucker et al. 2005) suggesting that tolerance to defocus may be ultimately limited by neural sampling. Our results show (see Figure 5.5) that natural aberrations in the eye cause severe decrease in the contrast and spatial resolution of retinal images, even in the absence of defocus (as it would occur if the hyperopic defocus measured using reflectometric techniques was caused by the small eye artefact and the eye was in fact nearly emmetropic). This is very different to what we found in the chick model (Chapter 3) where the optics was almost diffraction-limited both in normal eyes and myopic eyes treated with diffusers (removing the defocus term). While in normal conditions chicks have high contrast retinal images, mice have much poorer retinal images (with, and even without the hyperopic defocus, due to high order ocular aberration). As opposed to what happens in chicks, the high tolerance to defocus and to further degradation by diffusers seems to make eye growth more challenging to respond to changes in visual experience. Other complicating factors (Schmucker and Schaeffel 2004) are the slow ocular growth and a rod-dominated retina.

